Available online at www.sciencedirect.com

SciVerse ScienceDirect

Ceramics International 39 (2013) S701–S704

CERAMICS INTERNATIONAL

www.elsevier.com/locate/ceramint

Piezoelectric properties of lead free $BaTiO_3$ doped $0.9(Na_{0.52}K_{0.48})NbO_3$–$0.1AgLiTaO_3$ ceramics

Kyung-Su Lee, Jung-Hyuk Koh*

Department of Electronic Materials Engineering, Kwangwoon University, 139-701,Seoul, Korea

Abstract

0–3 mol% $BaTiO_3$ doped $0.9(Na_{0.52}K_{0.48})NbO_3$–$0.1AgLiTaO_3$ lead free piezoelectric ceramics have been prepared by employing the conventional mixed-oxide method. The doping effects of $BaTiO_3$ on the crystal structure, microstructure, and piezoelectric properties were investigated. The results indicate that the addition of the $BaTiO_3$ significantly influenced the crystal properties, microstructure, and electrical properties of NKN ceramics. The crystal structure of the 0–3 mol% $BaTiO_3$ doped $0.9(Na_{0.52}K_{0.48})NbO_3$–$0.1AgLiTaO_3$ lead free piezoelectric ceramics were investigated with X-ray diffraction analysis. Lattice parameters were investigated to extract the relationship between the structural properties and piezoelectric properties.

Keywords: D. $BaTiO_3$; Lead free piezoelectric; $(NaK)NbO_3$

1. Introduction

Ceramics based on lead zirconate titanate (PZT) system are the most important and have been widely used as piezoelectric materials because of their outstanding piezoelectric performance. However, the toxicity caused by lead evaporation leads to environmental pollution. Recently, lead free piezoelectric materials have been attracting increasing attention as new materials in place of PZT materials for sake of environmental protection. $(Na_{1-x}K_x)NbO_3$ (NKN) ceramic is a promising candidate material for lead free piezoelectric ceramics because of its good piezoelectric properties [1–3]. Hot pressed NKN ceramics have been reported to have good piezoelectric properties of 160 pC/N and electromechanical coupling coefficient (k_p) of 0.45 [4]. However, NKN ceramics are difficult to sinter by the conventional solid state method, because it can be melt when exposed to moisture. That is to say, the ceramic body of NKN solid solution turns to be porous and of deliquescence [5]. On the other hand, it is well recognized that $BaTiO_3$ is one of the typical ferroelectric materials showing large piezoelectricity, but its low Tc limits its piezoelectric applications. The addition of barium could improve its sinterability, lower its phase transitions temperature, and suppress the deliquescence. The morphotropic phase boundary (MBP) in lead-containing solid solutions such as $Pb(Ni,Nb)O_3$–$Pb(Zr,Ti)O_3$ (PNN–PZT) [6], $Pb(Mg,Nb)O_3$–$Pb(Zr,Ti)O_3$ (PMN–PZT) [7], $Pb(Ni_{1/3}Nb_{2/3})O_3$–$Pb(Zn_{1/3}Nb_{2/3})O_3$ (PNN–PZN) [8], and $Pb(Mg,Nb)O_3$–$PbTiO_3$ (PMN–PT) [9], plays a special role. A sample with its composition around the MPB shows excellent dielectric and piezoelectric properties. It was believed that the MPBs in PZT, PMN–PZT separate a tetragonal and a rhombohedral structure. However, recent research has revealed that there exists a low symmetric phase between the tetragonal and the rhombohedra phases [10]. The low symmetric phase is a monoclinic phase for the PZT and PMN–PT, and an orthorhombic phase for the PZN–PT [11,12]. Thus, the real MPB in the lead-containing solid solutions is a phase boundary between a monoclinic (orthorhombic) and a tetragonal structure. In developing high performance lead free piezoelectric materials, searching for phase transition has been considered as an effective method. $BaTiO_3$ is an excellent ferroelectric materials with high dielectric permittivity of 1700 and piezoelectric coefficient of 190 pC/N. However, low Curie temperature(115 °C) hindered versatile using of $BaTiO_3$ [13]. We believe that small contents of $BaTiO_3$ dopants with high

---

*Corresponding author. Tel.: +82 2 940 5162; fax: +82 2 915 0566.
E-mail address: jhkoh@kw.ac.kr (J.-H. Koh).

0272-8842/$ - see front matter © 2012 Elsevier Ltd and Techna Group S.r.l. All rights reserved.
http://dx.doi.org/10.1016/j.ceramint.2012.10.165

dielectric permittivity and piezoelectric coefficient can improve the piezoelectric properties of NKN ceramics.

In this paper, we will report our research on searching for the high performance piezoelectric properties at nearby phase transition area by using XRD method.

2. Experiments

In this study, 0–3 mol% $BaTiO_3$ doped $0.9(Na_{0.52}K_{0.48})NbO_3$–$0.1AgLiTaO_3$ (hereafter referred to as $BaTiO_3$ doped NKN–BT–ALT) ceramics were fabricated by the conventional mixed-oxide method. Na_2CO_3, K_2CO_3, Li_2CO_3, Nb_2O_5, Ta_2O_5, $BaCO_3$, TiO_2 and Ag_2O were employed as the starting materials. They were ball-milled for 24 h with ethyl alcohol with a zirconium ball. To obtain the high uniformity and crystal properties of the ceramics, a two-step calcination process was employed. At first, they were calcined at 850 °C for 5 h. The dried mixture was sieved to 100-mesh. These powders were mixed with a PVA binder. 12 mm diameter pellets were uniaxially pressed under 294 MPa and then sintered at 1100 °C with heating and cooling rates of 3 °C/min. For electrical measurements, silver paste was coated on both sides of the sintered samples and fired at 700 °C for 30 min to form electrodes. Dielectric permittivity and loss tangent of unpoled ceramics were measured using an impedance analyzer (HP4294A, Hewlett-Packard) at different frequency range from 1 kHz to 1 MHz in room temperature. The piezo- d_{33} meter (YE 2730A, USA) was used to measure the piezoelectric constant d_{33} at 110 Hz under 0.25 N. The piezoelectric ceramics were poled at 130 °C for 30 min at an applied electric field of 5 kV/mm. The electromechanical coupling factor k_p was calculated by using an impedance analyzer (HP 4194A) and that was calculated by measuring the anti-resonance and resonance frequency. The crystalline structure was investigated through X-ray diffraction (XRD) analysis employing a θ–2θ scans with a Cu-$K\alpha$ source radiation (Rigaku model *D*/Max-2500 V/PC, Japan). The microstructure was obtained with an SEM (Hitachi S-4300, Japan).

3. Results and discussions

Fig. 1 shows the θ–2θ X-ray diffraction patterns of the 0–3 mol% $BaTiO_3$ doped NKN–BT–ALT ceramics sintered at 1100 °C. X-ray diffraction analyses were carried out in order to know the structural properties of the samples. It can be seen that all the ceramics showed a perovskite structure. It states that the $BaTiO_3$ solution has diffused into the $0.9(Na_{0.52}K_{0.48})NbO_3$–$0.1AgLiTaO_3$ lattice and formed a solid solution. In this case, we suggest that Ba^{2+} occupy the empty A sites of the $0.9(Na_{0.52}K_{0.48})NbO_3$–$0.1AgLiTaO_3$ ceramics, and also Ti^{4+} occupy the empty B site of $0.9(Na_{0.52}K_{0.48})NbO_3$–$0.1AgLiTaO_3$. The inset of Fig. 1 exhibits the variation of (200) and (002) peak of $0.9(Na_{0.52}K_{0.48})NbO_3$–$0.1AgLiTaO_3$ ceramics near $2\theta = 45°$ with $BaTiO_3$ solution. The lattice parameters out of plane *c* and in plane *a* were calculated from Bragg's law and fitted by the *Nelson–Rilley* extrapolation function with the least mean square method.

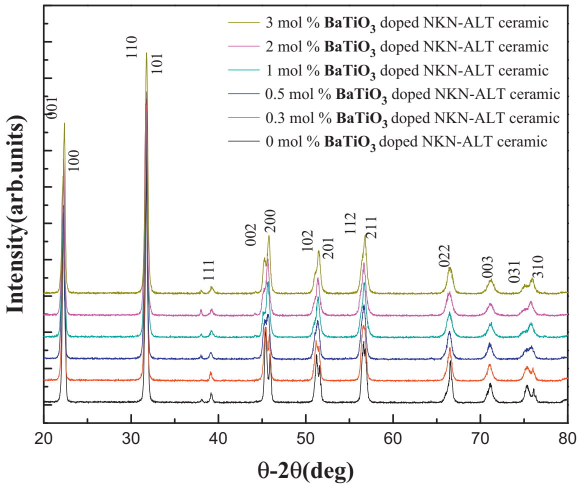

Fig. 1. X-ray diffraction $\theta-2\theta$ scans of 0–3 mol% $BaTiO_3$ doped $0.9(Na_{0.52}K_{0.48})NbO_3$–$0.1AgLiTaO_3$ ceramics.

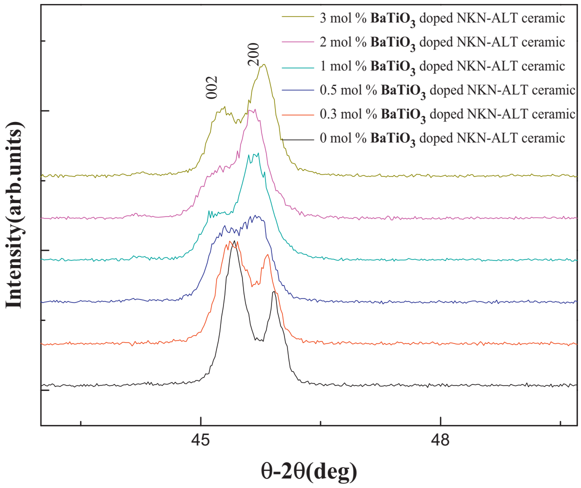

Fig. 2. X-ray diffraction θ–2θ scans of 0–3 mol% $BaTiO_3$ doped $0.9(Na_{0.52}K_{0.48})NbO_3$–$0.1AgLiTaO_3$ ceramics near the (002) and (200) planes.

$$\frac{C_{\cos\theta}-C_0}{C_0}=A\cos^2\theta\left(\frac{1}{\sin\theta}+\frac{1}{\theta}\right) \tag{1}$$

where $C_{\cos\theta}$ is an interplane distance calculated from the apparent Bragg peak position at 2θ and A is a fitting coefficient. The calculated lattice parameters *c* and *a* for 0–3 mol% $BaTiO_3$ doped NKN–BT–ALT ceramics varied from 3.948 to 4.03 Å and from 3.957 to 3.968 Å, respectively. We found that $BaTiO_3$ doped $0.9(Na_{0.52}K_{0.48})NbO_3$–$0.1AgLiTaO_3$ ceramics have a tetragonal structure.

Fig. 2 also reveals Bragg reflections for the (002) and (200) planes. According to the compositional change, the diffraction peaks slightly shift to a lower angle as the $BaTiO_3$ mol% increases. The 2θ peak positions of (002) for the 0–3 mol% $BaTiO_3$ doped $0.9(Na_{0.52}K_{0.48})NbO_3$–$0.1AgLiTaO_3$ specimens sintered at 1100 °C shifted from 45.46° (0 mol%) to

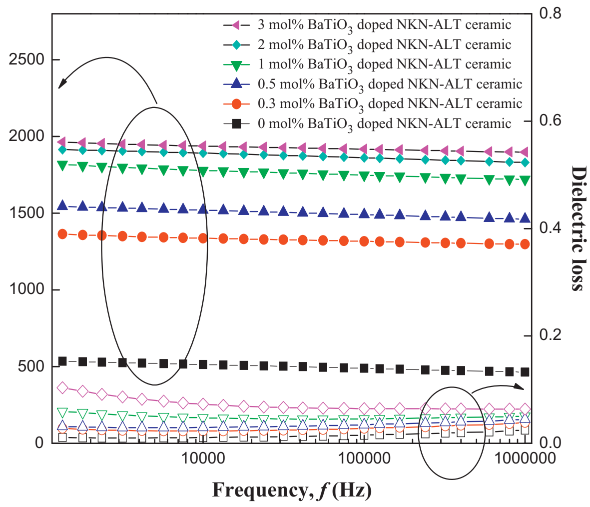

Fig. 3. Frequency dependent dielectric permittivity 0–3 mol% BaTiO$_3$ doped 0.9(Na$_{0.52}$K$_{0.48}$)NbO$_3$–0.1AgLiTaO$_3$ ceramics.

45.2° (3 mol%). This means that the lattice parameter *c* was increased as increasing BaTiO$_3$. 3 mol% BaTiO$_3$ doped 0.9(Na$_{0.52}$K$_{0.48}$)NbO$_3$–0.1AgLiTaO$_3$ ceramics had strong tetragonal properties, however the 0 mol% BaTiO$_3$ doped 0.9(Na$_{0.52}$K$_{0.48}$)NbO$_3$–0.1AgLiTaO$_3$ ceramics had weak tetragonal structures. As shown in the Fig. 3, mol% BaTiO$_3$ doped 0.9(Na$_{0.52}$K$_{0.48}$)NbO$_3$–0.1AgLiTaO$_3$ ceramics became tetragonal structure. Due to this increased tetragonality, we believe 3 mol% BaTiO$_3$ doped 0.9(Na$_{0.52}$K$_{0.48}$)NbO$_3$–0.1AgLiTaO$_3$ ceramics have high piezoelectric coefficient of 230 pC/N.

Fig. 3 illustrates the frequency dependent dielectric permittivity of the 0–3 mol% BaTiO$_3$ doped 0.9(Na$_{0.52}$K$_{0.48}$)NbO$_3$–0.1AgLiTaO$_3$ ceramics. The relative dielectric permittivities of the 0–3 mol% BaTiO$_3$ doped 0.9(Na$_{0.52}$K$_{0.48}$)NbO$_3$–0.1AgLiTaO$_3$ ceramics decreased as the frequency increased. For example, the permittivity of the 0 mol% BaTiO$_3$ doped 0.9(Na$_{0.52}$K$_{0.48}$)NbO$_3$–0.1AgLiTaO$_3$ ceramics decreased from 351.5 to 321.2 and from 100 kHz to 1 MHz. The dielectric dispersion of 0–3 mol% BaTiO$_3$ doped 0.9(Na$_{0.52}$K$_{0.48}$)NbO$_3$–0.1AgLiTaO$_3$ ceramics decreased as the doping contents increased. The calculated dielectric dispersion of the 3 mol% BaTiO$_3$ doped 0.9(Na$_{0.52}$K$_{0.48}$)NbO$_3$–0.1AgLiTaO$_3$ ceramics was 3.34%, while the 0 mol% BaTiO$_3$ doped 0.9(Na$_{0.52}$K$_{0.48}$)NbO$_3$–0.1AgLiTaO$_3$ ceramic was 8.54%, respectively. This behavior coincides relatively well with the BaTiO$_3$ properties, since BaTiO3 has the ferroelectric material with high dielectric permittivity of 1700 and loss tangent of 0.01. The ferroelectric materials with high loss tangent usually show large frequency dispersion [13].

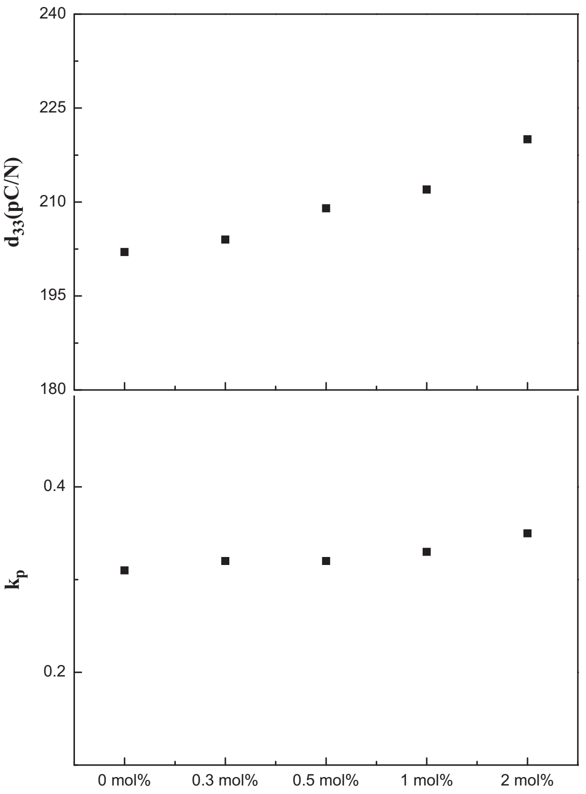

Fig. 4. Piezoelectric properties of 0–3 mol% BaTiO$_3$ doped 0.9(Na$_{0.52}$K$_{0.48}$)NbO$_3$–0.1AgLiTaO$_3$ ceramics.

Fig. 4 shows the piezoelectric properties of the 0–3 mol% BaTiO$_3$ doped 0.9(Na$_{0.52}$K$_{0.48}$)NbO$_3$–0.1AgLiTaO$_3$ ceramics. The piezoelectric properties such as piezoelectric charge coefficients d_{33} (202–230 pC/N) and electromechanical coupling coefficient k_p (33.3–38.1%) of the 0–3 mol% BaTiO$_3$ doped 0.9(Na$_{0.52}$K$_{0.48}$)NbO$_3$–0.1AgLiTaO$_3$ ceramics were exhibited. As shown in the figure, all parameters of piezoelectric charge coefficient d_{33}, electromechanical coupling coefficient k_p were increased as increasing the BaTiO$_3$. The electromechanical coupling coefficient k_p was calculated from these Eq. (2) The electromechanical coupling factor (k_p) is calculated by the following equation:

$$\frac{1}{k_p^2} \cong a \times \frac{f_r}{f_a+f_r} + b \tag{2}$$

where f_r is the resonance frequency, f_a is the anti-resonance frequency, $a=0.395$ and $b=0.574$ for electromechanical coupling factor (k_p) mode, respectively.

Fig. 5 shows the SEM micrographs of the 0–3 mol% BaTiO$_3$ doped 0.9(Na$_{0.52}$K$_{0.48}$)NbO$_3$–0.1AgLiTaO$_3$ ceramics sintered at 1100 °C. As shown in the figure, the grain size was increased, as the BaTiO$_3$ dopant. However, as the further increasing the BaTiO$_3$ contents, the grain size become decreased. For the 0–1 mol% BaTiO$_3$ doped 0.9(Na$_{0.52}$K$_{0.48}$)NbO$_3$–0.1AgLiTaO$_3$ ceramics, the grain has round type shape. However, as increasing the BaTiO$_3$ doping contents further, the grains become have rectangular shape.

4. Conclusions

The 0–3 mol% BaTiO$_3$ doped 0.9(Na$_{0.52}$K$_{0.48}$)NbO$_3$–0.1AgLiTaO$_3$ ceramics were prepared by the conventional mixed-oxide method. From the X-ray diffraction analysis, it was found that 0–3 mol% BaTiO$_3$ doped 0.9(Na$_{0.52}$K$_{0.48}$)NbO$_3$–0.1AgLiTaO$_3$ ceramics have tetragonal structure. Also, we found that 3 mol% BaTiO$_3$ doped 0.9(Na$_{0.52}$K$_{0.48}$)NbO$_3$–0.1AgLiTaO$_3$ ceramics have relatively high

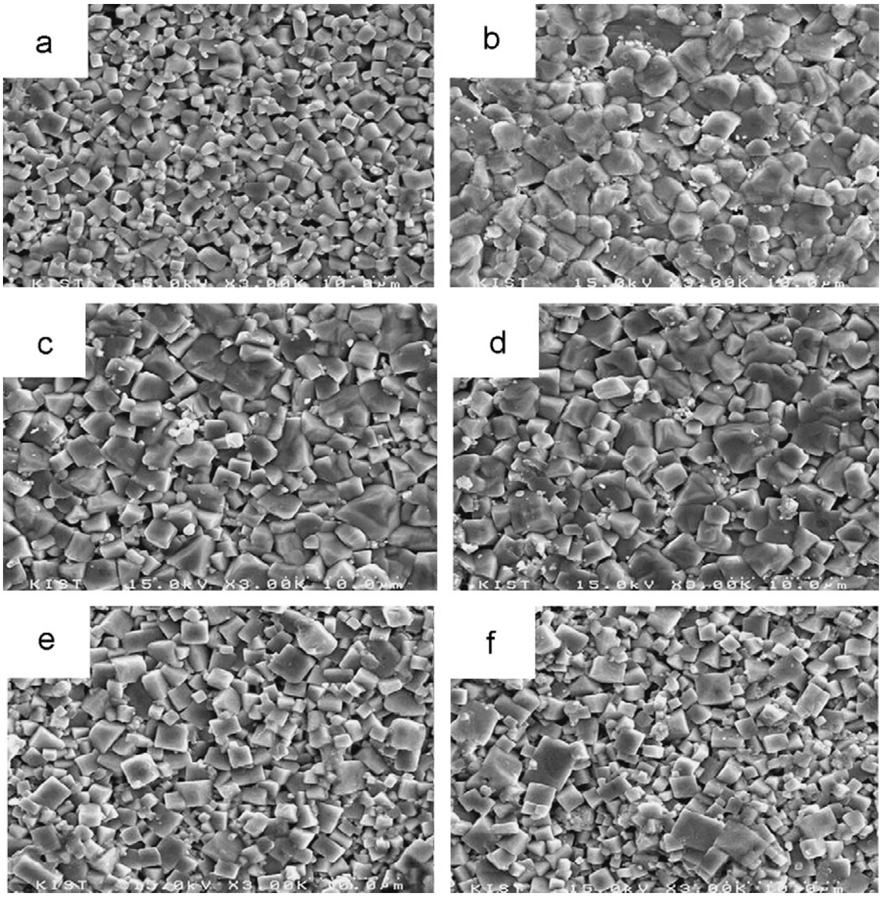

Fig. 5. Scanning electron micrograph of sintered surface of 0–3 mol% $BaTiO_3$ doped $0.9(Na_{0.52}K_{0.48})NbO_3$–$0.1AgLiTaO_3$ ceramics. (a)$BaTiO_3$ 0 mol%, (b)$BaTiO_3$ 0.3 mol%, (c)$BaTiO_3$ 0.5 mol%, (d)$BaTiO_3$ 1 mol%, (e)$BaTiO_3$ 2 mol% and (f)$BaTiO_3$ 3 mol%.

piezoelectric coefficient (d_{33}) of 230 pC/N and electromechanical coupling coefficient (k_p) of 0.36. These excellent piezoelectric properties mean this lead free $BaTiO_3$ doped $0.9(Na_{0.52}K_{0.48})NbO_3$–$0.1AgLiTaO_3$ ceramics can be an alternative lead free piezoelectric material.

Acknowledgments

This work was financially supported by the Basic Science Research program, through the National Research Foundation of KOREA (NRF), funded by the Ministry of Education, Science and Technology (grant number 2010–0011536), and the National Research Foundation of Korea(NRF) grant funded by the Korea government(MEST) (No. 2011-0029625)

References

[1] G. Shirane, R. Newnham, R. Pepinsky, Dielectric properties and phase transitions of $NaNbO_3$ and $(Na,K)NbO_3$, Physical Review 96 (1954) 581–588.

[2] L. Egerton, D.M. Dillon, Piezoelectric and Dielectric properties of ceramics in the system potassium–sodium niobate, Journal of the American Ceramic Society 42 (1959) 438–442.

[3] R.E. Jaeger, L. Egerton, Hot pressing of potassium–sodium niobates, Journal of the American Ceramic Society 45 (1962) 209–213.

[4] G.H. Haertling, Properties of hot-pressed ferroelectric alkali niobate ceramics, Journal of the American Ceramic Society 50 (2000) 329–330.

[5] A. Reisman, F. Holtzberg, S. Triebwasser, M. Berkenblit, Preparation of pure potassium metaniobate, Journal of the American Chemical Society 78 (1956) 719–721.

[6] J. Qiu, J. Tani, N. Yanada, Y. Kobayashi, Fabrication of $Pb(Nb,Ni)O_3$–$Pb(Zr,Ti)O_3$ piezoelectric ceramic fibers by extrusion of a sol-powder mixture, Japan Journal of Intelligent Material Systems and Structures 15 (2004) 643–653.

[7] J.H. Koh, S.J. Jeong, M.S. Ha, S.J. Song, Aging of piezoelectric properties in $Pb(MgNb)O_3$–$Pb(ZrTi)O_3$ multilayer ceramic actuators, Journal of Applied Physics 96 (2004) 544–548.

[8] S.T. Chung, K. Nagata, H. Igarashi, Piezoelectric and dielectric properties of $PbTiO_3$–$PbZrO_3$–$Pb(Ni,Nb)O_3$–$Pb(Zn,Nb)O_3$ system ceramics, Ferroelectrics 94 (1989) 243–247.

[9] S.W. Choi, R.T.R. Shrout, S.J. Jang, A.S. Bhalla, Dielectric and pyroelectric properties in the $Pb(Mg_{1/3}Nb_{2/3})O_3$–$PbTiO_3$ system, Ferroelectrics 100 (1989) 29–38.

[10] B. Noheda, D.E. Cox, G. Shirane, R. Guo, B. Jones, L.E. Cross, Stability of the monoclinic phase in the ferroelectric perovskite $PbZr_{1-x}Ti_xO_3$, Physical Review B 63 (2000) 014103.

[11] D. La. Orauttapong, B. Noheda, Z.-G. Ye, P.M. Gehring, J. Touloues, D.E. Cox, G. Shirane, Phase diagram of the relaxor ferroelectric $(1-x)Pb(Zn_{1/3}Nb_{2/3})O_3$–$xPbTiO_3$, Physical Review B 65 (2002) 144101.

[12] B. Noheda, D.E. Cox, G. Shirane, J. Guo, Z.–G. Ye, Phase diagram of the ferroelectric relaxor $(1-x)PbMg_{1/3}Nb_{2/3}O_{3-x}PbTiO_3$, Physical Review B 66 (2002) 054104.

[13] H. Jaffe, Piezoelectric ceramics, Journal of the American Ceramic Society 41 (1958) 494–498.